Wintertime transport processes in the Gulf of Naples investigated by HF radar measurements of surface currents

M. Menna[1], A. Mercatini[1], M. Uttieri[1][2], B. Buonocore[1] and
E. Zambianchi[1]

[1] *Dipartimento di Scienze per l'Ambiente, "Parthenope" University*
    Centro Direzionale di Napoli - Isola C4, 80143 Napoli, Italy
[2] *AMRA scarl-Competence Center for Analysis and Monitoring of Environmental Risk*
    Via Nuova Agnano 11, 80125 Napoli, Italy

Summary. — Transport processes play a fundamental role in regulating the water renewal in coastal systems. The Gulf of Naples (Southern Tyrrhenian Sea) is a highly urbanised area, receiving pollutant discharges and terrestrial inputs that may reside inside the basin. For this reason, understanding the processes governing coast-offshore transport is of paramount importance for the welfare of the ecosystem and the sustainable exploitation of environmental resources. In this work, we analyse the wind-driven transport over lags of three days in winter reconstructing the basin scale surface circulation by means of High-Frequency radars and evaluating its dependence on wind circulation. Simulations of particle exchange between a coastal and an offshore area have been carried out, outlining the strong relationship between particle fate and circulation structures. Results are interpreted in terms of residence times and possible aggregative areas in the Gulf of Naples.

PACS 92.10.Sx – Coastal, estuarine, and near shore processes.

1. – Introduction

The dynamics of coastal ecosystems are strongly dependent on water mass circulation and on transport processes, which may affect the distribution of hydrological characteristics as well as that of different dissolved or suspended substances. In particular, transport processes determine particle exchange between adjacent basins and/or sub-basins, thus affecting the effectiveness of water renewal mechanisms. The importance of their assessment is even more evident in the case of densely inhabited coastal areas, where pollutants and other man-derived products may accumulate.

The Gulf of Naples (GoN hereinafter), a marginal basin of the Southern Tyrrhenian Sea, is a text-book example of rectangular semi-enclosed basin [1]. It is in direct communication with the Tyrrhenian Sea through its main aperture ("Bocca Grande"), and with the Gulfs of Salerno and Gaeta respectively through the "Bocca Piccola" and the Ischia/Procida Channels (fig. 1). The basin is interested by an intense anthropic activity [2,3]: the coast extends for 195 km (including the islands of Capri, Ischia and Procida), with approximately 30 ports and over 300 major maritime constructions [3].
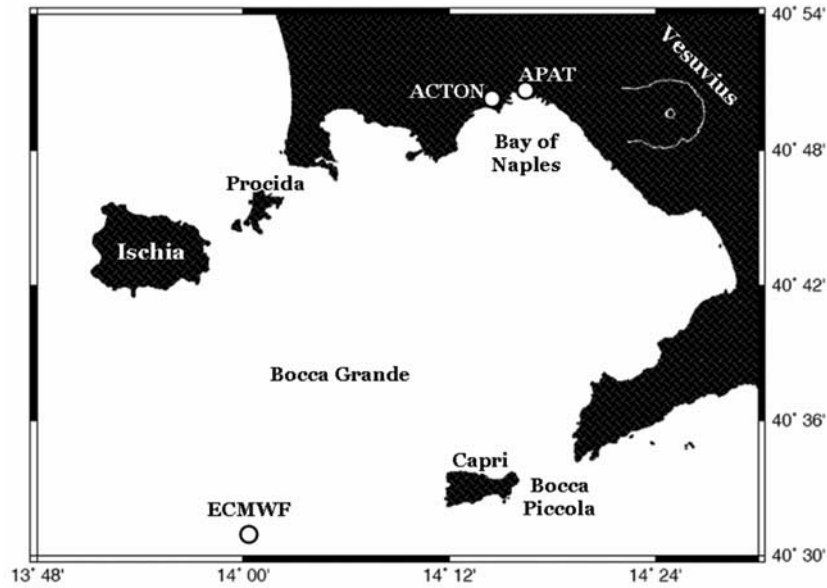
Fig. 1. – Map of the Gulf of Naples with the location of the two weather stations (Acton and Apat) and of the ECMWF grid point.

Several water masses are present in this area [4] which, based on photophysiological and hydrological parameters, can be classified as a Case I water region [5,6]. The GoN can be divided in two areas: the interior of the Gulf, with hydrological characteristics similar to the Tyrrhenian Sea, including oligotrophic traits [7]; and a nearshore region (the so-called Bay of Naples) subject to coastal variability and occasionally affected by land inputs [8,9].

The circulation of the Gulf of Naples (GoN) is the result of the non-linear superimposition of motion components evolving over different spatial and temporal scales [10]. Two spatially different classes of forcings can be identified: remote and local ones [1]. The primary remote forcing is the circulation of the Southern Tyrrhenian Sea [11], while among the local factors the most relevant is wind stress [1,12,13], generating currents up to one order of magnitude greater than the mean basin circulation [12]. Surface circulation in the GoN is strongly influenced by the shelter effect of Vesuvius volcano (elevation: 1,281 m) [1,12,13], while modelling studies demonstrate that bottom topography affects the deeper circulation [1,14]. Surface currents show a periodicity of 3-7 days all year round, with an overlaid inertial oscillation in the presence of a well-developed thermocline, a condition typical of summer and fall months [13]. Smaller contributions derive from semidiurnal and diurnal tidal components as well, even though never substantially representing a relevant energetic input [10].

The present work is aimed at fostering the comprehension of short-time wind-induced transport processes in the GoN and the associated coast-offshore exchanges. To achieve our goal we first investigate the characteristic wind regime acting on the basin, looking at both yearly and seasonal patterns. We then reconstruct the synoptic winter-time basin-scale surface circulation using a High-Frequency (HF) coastal radar system, and correlating the observed surface velocity field with meteorological measurements collected

by two weather stations and with surface wind data derived from a numerical model. Finally, we focus on surface transport by simulating the exchange of purely advected Lagrangian particles released from a coastal and an offshore sector of the basin. Both circulation features and particle exchange depend, over periods of three days, on the wind conditions acting over the basin, with drastic differences in terms of residence times and total tracer concentration depending on wind-induced circulations. Our results highlight specific circulation patterns in the GoN and provide a rationale for the study of potential consequences of the release of toxic or pollutant substances in the GoN.

2. – Observation sites and meteorological data set

The starting point of this work is the analysis of wind data collected in the GoN region during the 2002-2006 period to identify the typical wind directions and intensities. The data set is composed by measurements recorded by two weather stations localised in the urban area of Naples: 1) the Acton station (latitude $40°30.19'$ N, longitude $14°15.21'$ E, anemometric sensor height 16 m a.m.s.l.), belonging to the monitoring network managed by the Department of Environmental Sciences of the "Parthenope" University of Naples; 2) the Apat station (latitude $40°50.38'$ N, longitude $14°16.15'$ E, anemometric sensor height 10 m a.m.s.l.), placed in the harbour of Naples and managed by the Italian National Agency for Environmental Protection and Technical Services (APAT). APAT data are freely downloadable from the website `www.idromare.com` and are part of the meteorological-tidal Italian National Tide Gauge Network. In order to compare local and basin-scale wind features, we have also utilized 10 m a.m.s.l. velocities produced by the ECMWF (European Centre for Medium-Range Weather Forecasts) atmospheric model relative to the closest model gridpoint ($40°30.00'$ N, $14°00.00'$ E). Figure 1 shows the location of the three observation sites.

Time series from each data set have been statistically characterised with the box-plot method [15] to evaluate possible year-to-year variations in wind measurements. Each box contains lines representative of the lower, median and upper quartiles; the whiskers, extending from each end of the box, represent the rest of the data outside the interquartile range. Outliers are graphed as single data points outside the whiskers. Samples are considered statistically similar when the dispersion of data around the median (*i.e.* the interquartile range) is comparable and overlapping.

3. – Wind speed and direction, sea level pressure data

For the entire observation period (2002-2006), we show wind rose diagrams for the two weather stations and for the ECMWF data. In these diagrams, wind directions are divided into 16 sectors of 22.5 grades; the length of the bins corresponds to the percentage frequency of wind blowing from a given direction, while grey levels indicate different intervals of wind intensity. Wind roses highlight the dominant wind patterns and their yearly and seasonal peculiarities.

In addition, since in this work we focus on the wind-induced transport processes during the winter period, which deserves peculiar attention since it is crucial for the development of circulation structures affecting oceanographic and ecosystem dynamics, the monthly wind data-sets have been analyzed in conjunction with the corresponding time series of sea level pressure, in order to evaluate the short-term wind-field variability associated with the passage of low-pressure systems.

Fig. 2. – Coverage of the HF radar system in the Gulf of Naples, with the location of the two antennas (Portici and Massa Lubrense) and of the central site (Napoli).

4. – The coastal radar system

HF radar systems provide synoptic basin scale surface current measurements (*e.g.*, [16, 17]). A SeaSonde system manufactured by CODAR O. S. Ltd. (USA), based on the original set-up described in [18] and comprising two remote HF radar stations and a central control site, is installed in the GoN (fig. 2). HF radars measure surface currents using the Bragg backscattering of electromagnetic pulses from a rough moving sea surface [19], where the roughness is due to the presence of surface gravity waves superimposed on the current field, and the actual current measurement is drawn from the Doppler shift of the signal. Measured currents are typically representative of the first meter of water column. The accuracy of current estimates and the working ranges of such systems are susceptible to a variety of potential errors, which must be carefully taken into account for an efficient use (*e.g.*, [20]). The interested reader can refer to the excellent reviews [21, 22] for more technical details on HF radar systems. A recent work [23] has also highlighted the potential of HF radar systems as a monitoring instrument for tsunami detection.

A CODAR HF radar system has been operating in the GoN since October 2004; the configuration adopted covers almost entirely the basin (fig. 2), with a range of approximately 30 km from the coast and a covered area of nearly 525 km^2. Technical specifications of the system utilised are provided in table I. The two remote sites collect hourly averaged fields of surface currents, with a sweep band width of 150.147 kHz resulting in a radial range step of 0.999 km. Radial maps are then merged together over a regular grid of side length equal to 1.250 km providing a real time synoptic, basin-scale map of surface current direction and intensity.

TABLE I. – *Technical features of the HF radar system installed in the Gulf of Naples.*

Radial maps acquisition	
Frequency	25.2–25.4 MHz
Sweep rate	2 Hz
Samples per sweep	2048
Bandwidth	150.147 kHz
Range step	0.999 km
Range	~ 30 km
Wavelength	12 m
Radial maps combine options	
Grid spacing	1.250 km
Averaging radius	2.0 km
Distance angular limit	25° GDOP limit
Current velocity limit	80 cm s^{-1}

5. – Cross-correlation between surface currents and wind stress

The main aim of the present work is to understand how short-term wintertime transport processes are driven by local wind forcings. To characterise the role of wind stress in guiding surface circulation, we use the cross-correlation function $X_{cc}(-\tau)$ [24] to evaluate how the surface current at a generic time t depended on the wind stress acting at the same moment (t) and at previous times $(t - \tau)$. In particular, we cross-correlated the direction (d), the zonal (u) and the meridional (v) components of sea surface velocities and wind stress according to

$$(1) \qquad X_{ccd}(-\tau) \equiv \overline{d_s(t)d_w(t - \tau)},$$

$$(2) \qquad X_{ccu}(-\tau) \equiv \overline{u_s(t)u_w(t - \tau)},$$

$$(3) \qquad X_{ccv}(-\tau) \equiv \overline{v_s(t)v_w(t - \tau)},$$

where the subscripts s and w respectively refer to sea and wind components. It is worth underlining that, unlike the autocorrelation function, cross-correlation is not a symmetric function of the time lag τ [24]. Surface current data in a given grid point have been cross-correlated with the hourly updated Acton wind measurements, taken as representative of the basin-scale wind conditions. Wind stress was evaluated as

$$(4) \qquad \begin{aligned} u_w &= \rho_a c_d |U| u \\ v_w &= \rho_a c_d |U| v \end{aligned}$$

where $U = (u_w, v_w)$ is the wind velocity, ρ_a is a reference air density $(1.3 \, \text{kg} \, \text{m}^{-3})$, and c_d is the drag coefficient calculated as in [25]:

$$(5) \qquad \begin{cases} c_d = 10^{-3}, & |U| \leq 6 \, \text{m} \, \text{s}^{-1}, \\ c_d = (0.61 + 0.063 \cdot |U|)/10^{-3}, & 6 \, \text{m} \, \text{s}^{-1} < |U| \leq 22 \, \text{m} \, \text{s}^{-1}, \\ c_d = 2 \times 10^{-3}, & 22 \, \text{m} \, \text{s}^{-1} < |U|. \end{cases}$$
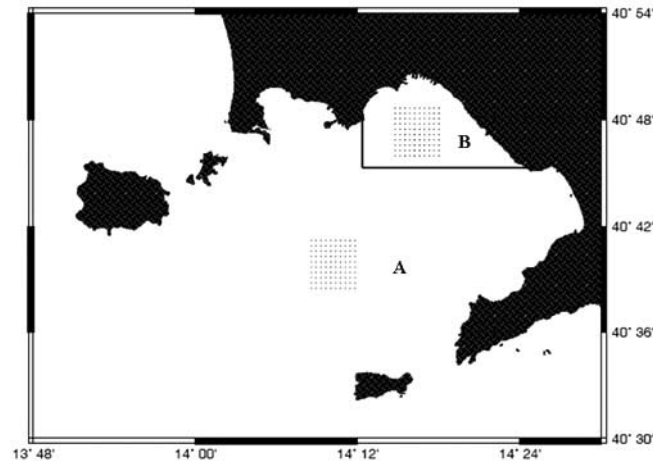
Fig. 3. – Location of the deployment grids in the offshore (A) and coastal (B) sectors.

Cross-correlations have been carried out for both the offshore sector of the GoN and for an inner sub-basin (Bay of Naples) defined in the Introduction (fig. 3). This approach permits to highlight the relationship existing between large- and small-scale observed surface circulation and the wind pattern over the area of the GoN.

6. – Characterization of transport processes

The surface transport of Lagrangian tracers has been simulated numerically; the velocity field used to advect particles is represented by the surface currents measured by the HF radar system. Tracer particles are assumed as conservative and purely passive; these assumptions allow to highlight the role of circulation on dispersion, disregarding diffusion and changes in the inherent physical characteristics of the tracer. The movement of each particle is reconstructed, using a specifically conceived Java routine, by interpolating every 30 minutes the CODAR data for each grid point and calculating the position of each particle starting from the coordinates of the previous time step and interpolating them using the velocities of the four nearest-neighbouring grid points.

For each investigated period two distinct release grids are used, one for the offshore sector and the other for the coastal one (fig. 3). Each grid comprises 100 particles homogeneously distributed over a 5×5 km lattice. This allows to quantify the exchanges between the two regions and the evaluation of potential coast-offshore transport, as well as the identification of possible retention mechanisms. Preliminary analysis showed that the number of particles launched provided a statistically reliable set of data on which to base our observations. From the period investigated (February 2005 and January 2007) we selected a set of three-day periods (8 for NE winds, 5 for SW winds) over which the wind conditions were relatively stable. The choice of this time duration also allowed us to perform direct comparisons with *in situ* data obtained during oceanographic cruises [12].

Following [26], we quantify transport processes by means of the total concentration $Q(t)$ and of the residence time T of the released particles. As particles are assumed to be conservative, their concentration corresponds to the average concentration of tracer in the release area [27]. We estimate the normalized number of particles which, at time

t, are still inside the release area as

$$(6) \qquad Q(t) = \frac{N(t)}{N(0)},$$

$N(t)$ being the number of particles present at t and $N(0)$ the pool of originally launched tracers. The residence time, *i.e.* the time spent by a particle in the release area before exiting it, is estimated as

$$(7) \qquad T = \lim_{t \to \infty} T^*(t)$$

with

$$(8) \qquad T^*(t) = tQ(t) + \sum_{i=1}^{N_e(t)} \frac{t_{ei}}{N(0)},$$

where $N_e(t) = N(0) - N(t)$ is the number of particles which have already abandoned the release area at time t, and t_{ei} represents the time taken by the i-th particle to exit the launch sector. Preliminary analysis showed that when a particle exited the original domain it did not re-enter it again over the investigated time span, making unnecessary the definition a buffer zone (*e.g.*, [28]). In the present work, the parameter $Q(t)$ has been evaluated for both offshore and coastal sectors, while the residence times have been evaluated exclusively for the inner area. Moreover, particles completely abandoning the GoN through one of the boundaries are assumed as still present in the offshore sector.

7. – Results

Figure 4 shows the four-year (2002-2006) wind roses for the three data sets used (Acton, Apat, ECMWF). The two weather stations located inside the GoN show, on an annual basis, wind prevalently blowing from the NE and SW quadrants. ECMWF data agree with the meteorological stations for the NE quadrant; however, south-westerly winds recorded by the two weather stations are replaced by W,W-SW and W-NW winds. This shift in direction is most likely due to the position of the weather stations which, owing to orographic barriers, are sheltered from westerly winds. Overall, ECMWF wind intensities appear to be slightly higher than those recorded at the two land sites, a discrepancy already noticed in other similar works (*e.g.*, [29]). The boxplots in fig. 5 show that, for each data set used, no major inter-annual difference is observed in terms of direction and intensity, supporting the existence of a recurrency in the observed patterns.

Seasonal wind analysis (fig. 6) confirms the presence of two principal directions. In this work we refer to the meteorological classification of seasons as given in [30]. For the two internal stations, the predominant and most intense winds come from NNE and NE directions during winter months (December-February), with maximum velocities in the range 8–$10 \, \mathrm{m \, s^{-1}}$; wind episodes from S and SSW are much less frequent but more intense ($\geq 10 \, \mathrm{m \, s^{-1}}$). In the summer period (June-August) winds are generally weaker than during the rest of the year; the main direction with the most intense wind ($\geq 6 \, \mathrm{m \, s^{-1}}$) is from SSW. In spring (March-May) and autumn (September-November) the principal directions are along the NE-SW axes. In particular, in spring the strongest winds are
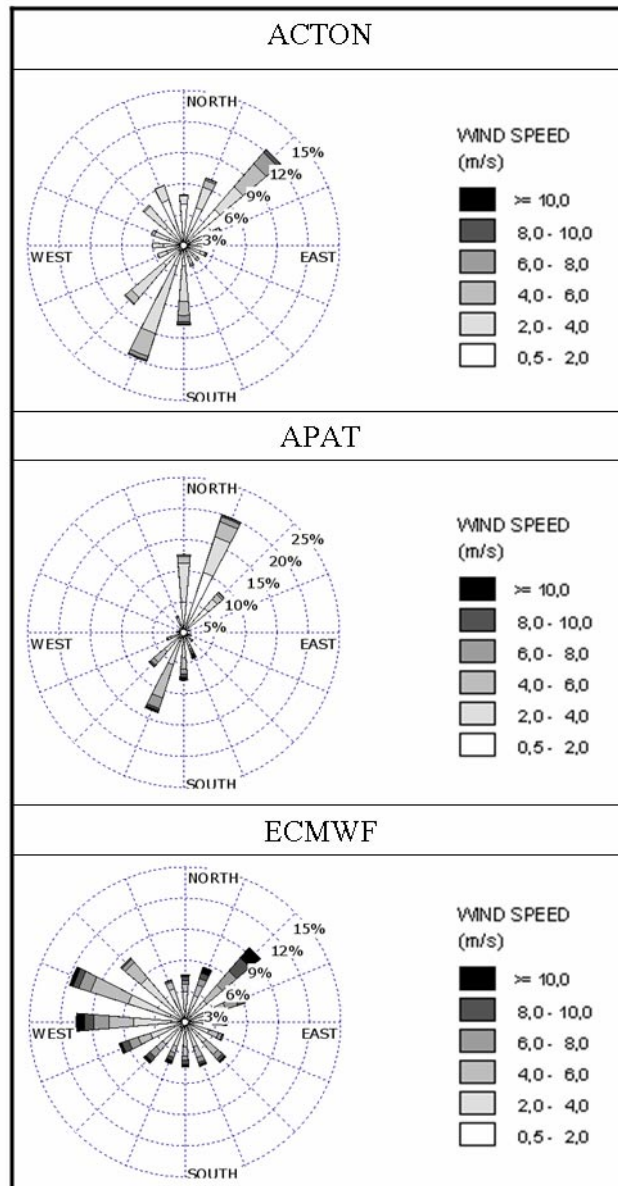
Fig. 4. – Wind rose diagrams for the three data sets used in this work, relative to the years 2002 through 2006. Calm periods (0.0–0.5 m/s) for Acton, Apat and ECMWF respectively account for 10.6%, 9.6% and 1.1%.
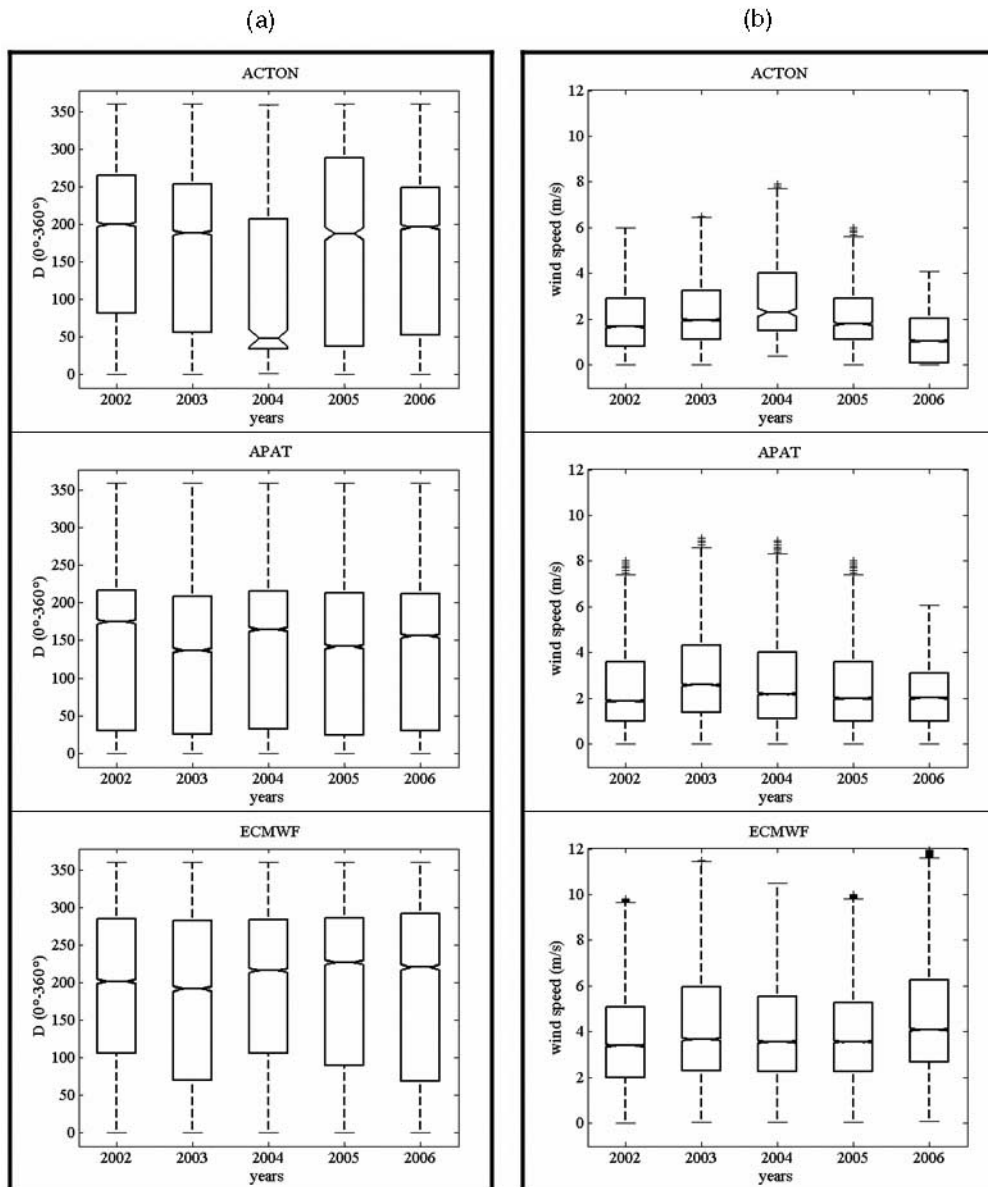
Fig. 5. – Boxplots of wind direction (a) and intensity (b) for the three data sets. Dispersions around the medians are always comparable and overlapping, indicating that the wind characteristics remain constant over the observation period.

from SSW (8–$10\,\mathrm{m\,s}^{-1}$) and S ($\geq 10\,\mathrm{m\,s}^{-1}$), whereas in autumn winds $\geq 6\,\mathrm{m\,s}^{-1}$ are recorded from SSW.

The seasonal ECMWF rose diagrams (fig. 6) confirm the main winds blowing from W, W-NW and W-SW. These winds are in particular present during spring-summer months, and are characterised by high intensity, sometimes higher than $10\,\mathrm{m\,s}^{-1}$. During winter-
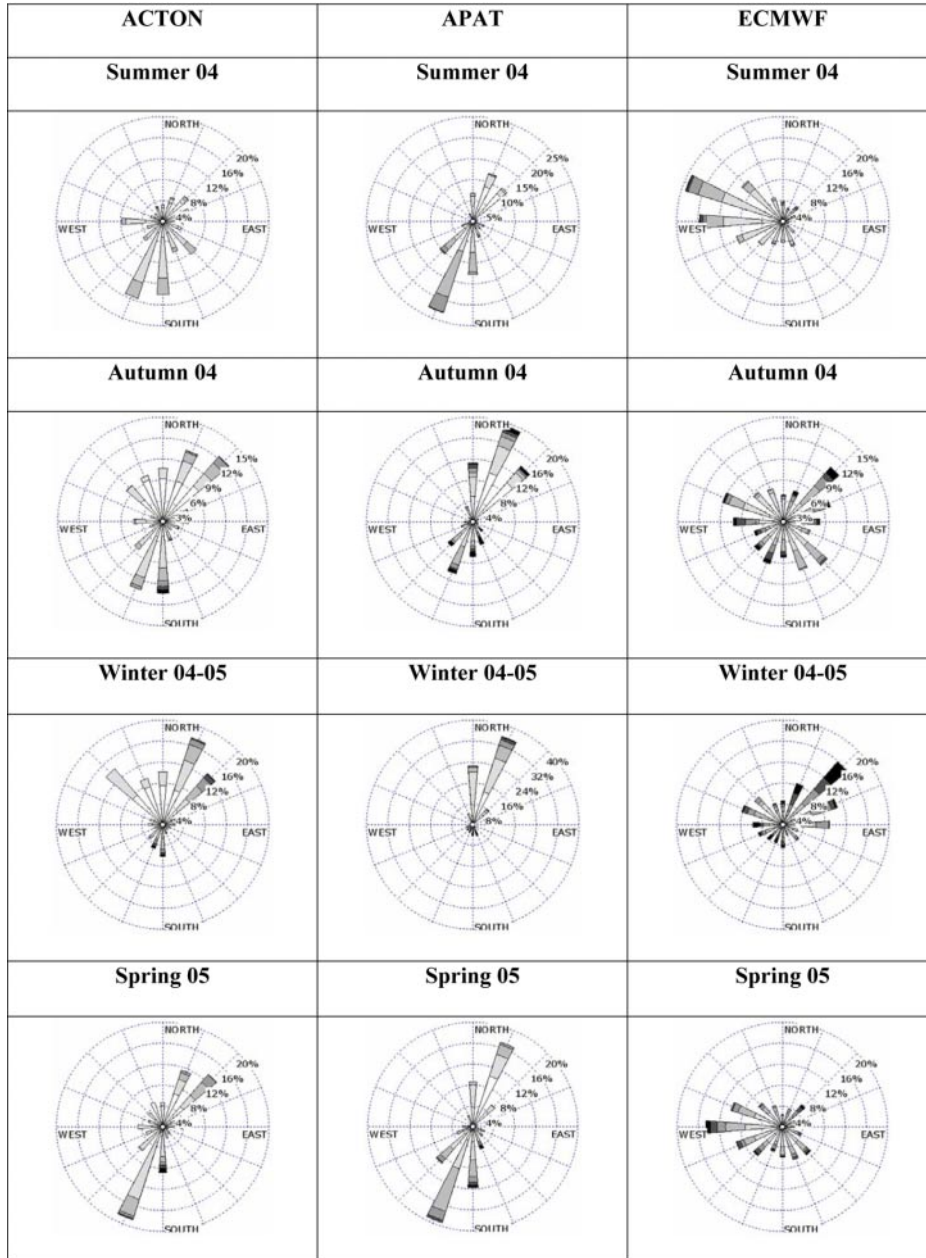
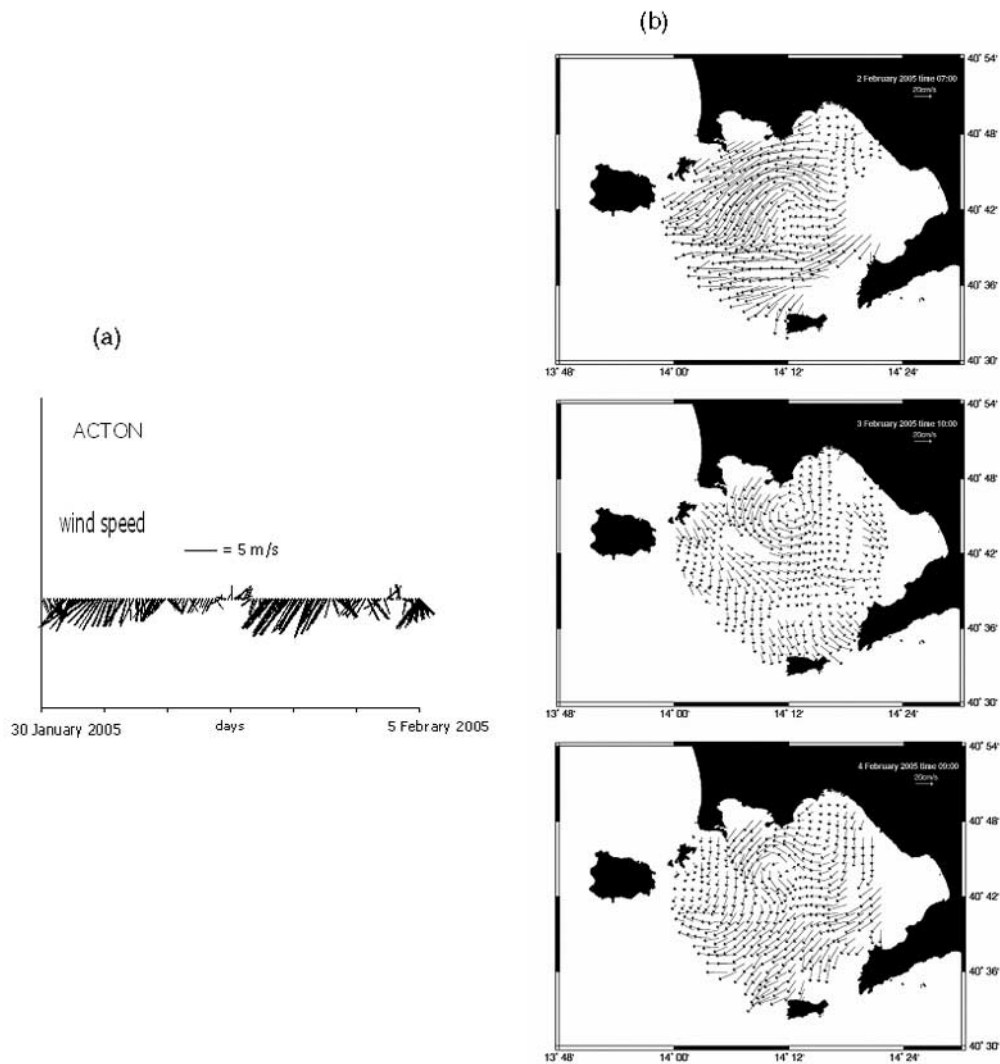Fig. 6. – Seasonal wind rose diagrams for the three data sets over the period summer 2004-spring 2005.

Fig. 7. – a) Wind speed and direction measured at the Acton station in the period 30 January-5 February 2005. b) Corresponding sea surface circulation, showing the presence of a characteristic coast-offshore jet associated with easterlies.

autumn months, the highest intensities are observed from the NE direction and are included in the interval 8–10 and $\geq 10\,\mathrm{m\,s^{-1}}$.

Figure 7a shows wind direction and intensity measured by the Acton weather station in early February 2005, whereas fig. 8a shows the wind data collected in January 2007. The corresponding circulation in the GoN (figs. 7b and 8b) shows markedly different features depending on the wind direction. A jet almost perpendicular to the coast and directed offshore towards the "Bocca Grande" (similar to those reported in [31, 32]) is typically associated with easterlies, with a secondary circulation in the remaining part of the basin characterised by gyres and coast-approaching currents. This pattern is in full agreement with previous *in situ* observations [12] as well as model results [1,
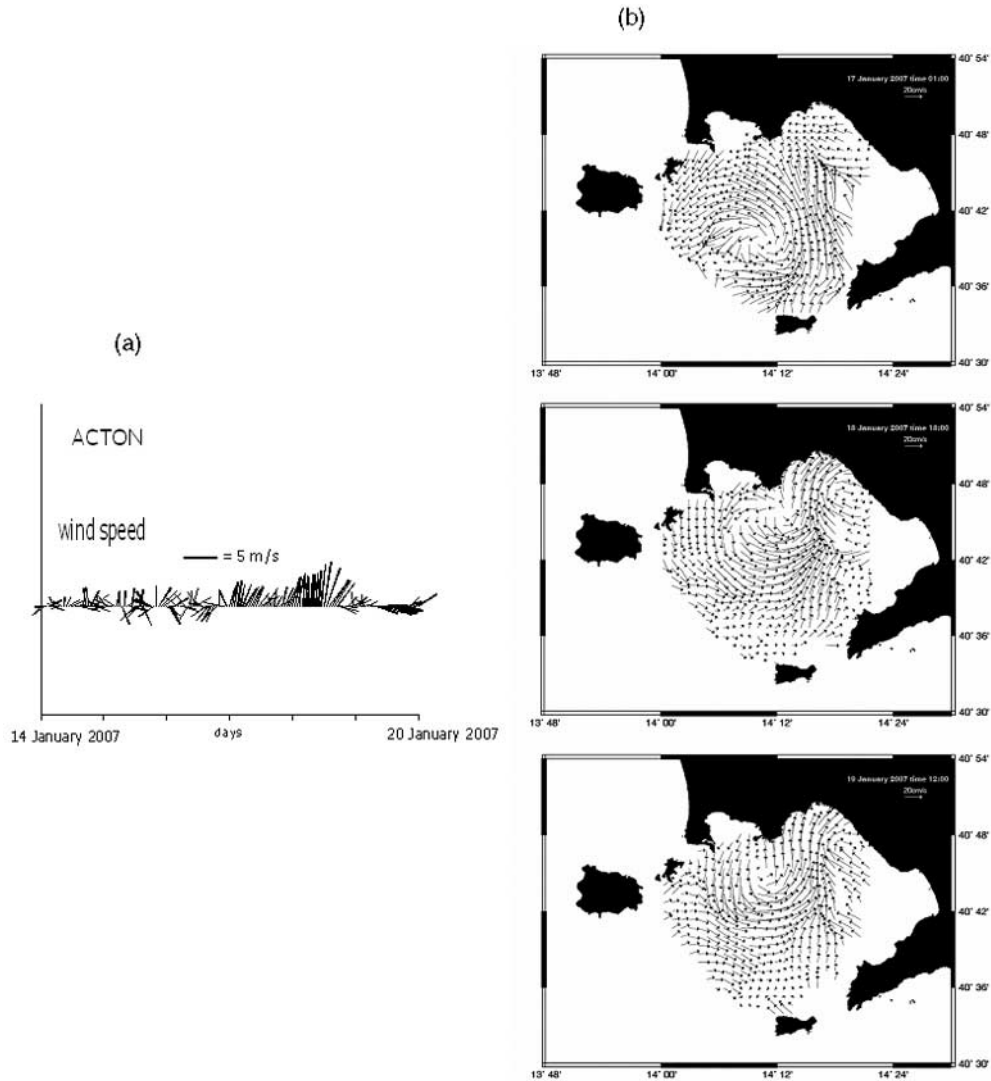
Fig. 8. – a) Wind speed and direction measured at the Acton station in the period 14-20 January 2007. b) Corresponding sea surface circulation, showing the presence of cyclonic and anticyclonic structures.

14]. The coastal jet displays latitudinal shifts inside the basin as a function of the sheltering effect by the Vesuvius volcano, which can deviate the wind channelling it over the basin [13]. The pattern of surface currents associated with westerlies (fig. 8b) is, on the contrary, characterised by the presence of recirculation structures, with both cyclonic and anticyclonic gyres at basin and sub-basin scales, confirming the numerical simulations by [1] and [14].

The cross-correlation with Acton data shows that, in the case of easterly winds (fig. 9a), both the zonal and meridional velocity components of wind and sea surface, as
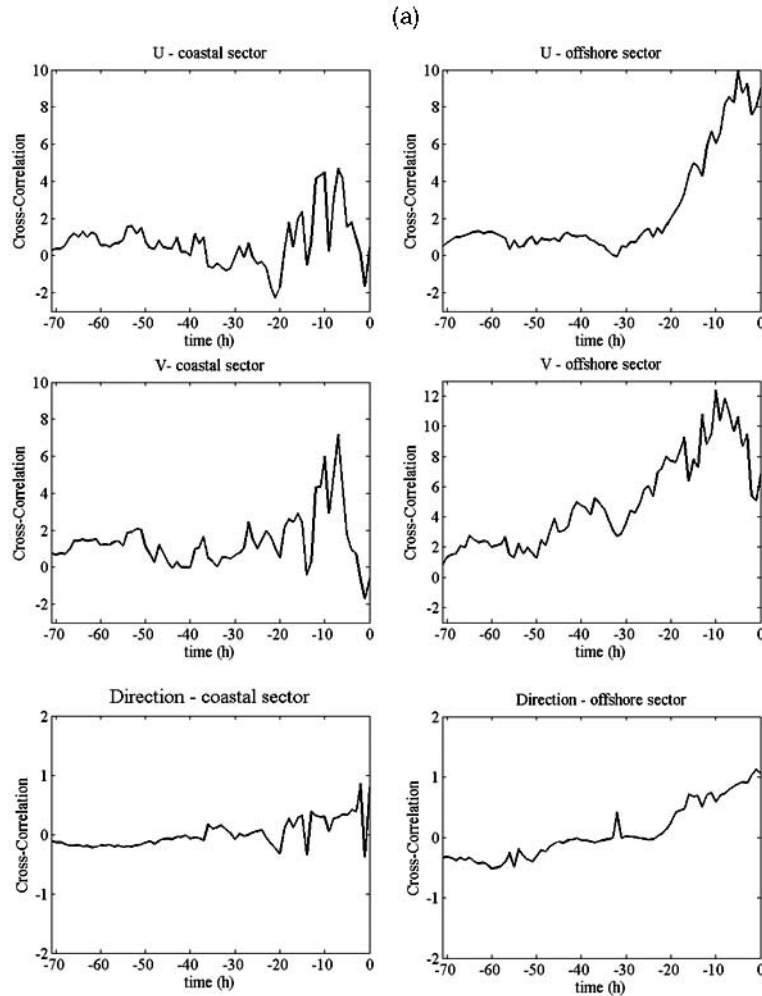
(a)

Fig. 9. – Cross-correlations between direction, zonal (u) and meridional (v) components of the wind stress and sea surface current for easterly (a) and westerly winds (b). In the case of easterly winds, the surface circulation is relatively well correlated with the wind stress, whereas in the case of westerlies neither the offshore nor the inner part of the GoN show any remarkable correlation with the wind stress.

well as their directions, are well correlated for almost 10 h. This result holds for both the offshore and the coastal sectors. When winds come from SW, in the offshore and coastal sectors wind and sea surface current directions are cross-correlated for just a few hours in the directions (2-3 h on average, see fig. 9b), whilst velocity components are not correlated. For both easterlies and westerlies, Acton results were confirmed by cross-correlating sea surface velocity fields with data obtained from ECMWF station (results not shown).

Just like the circulation, also transport processes are strongly dependent on wind conditions. During NE wind episodes, the 98% of offshore released particles remains in open waters, rapidly being carried by the coastal jet, and often approaching the external boundaries of the GoN. By contrast, particles originated in the inner coastal

(b)
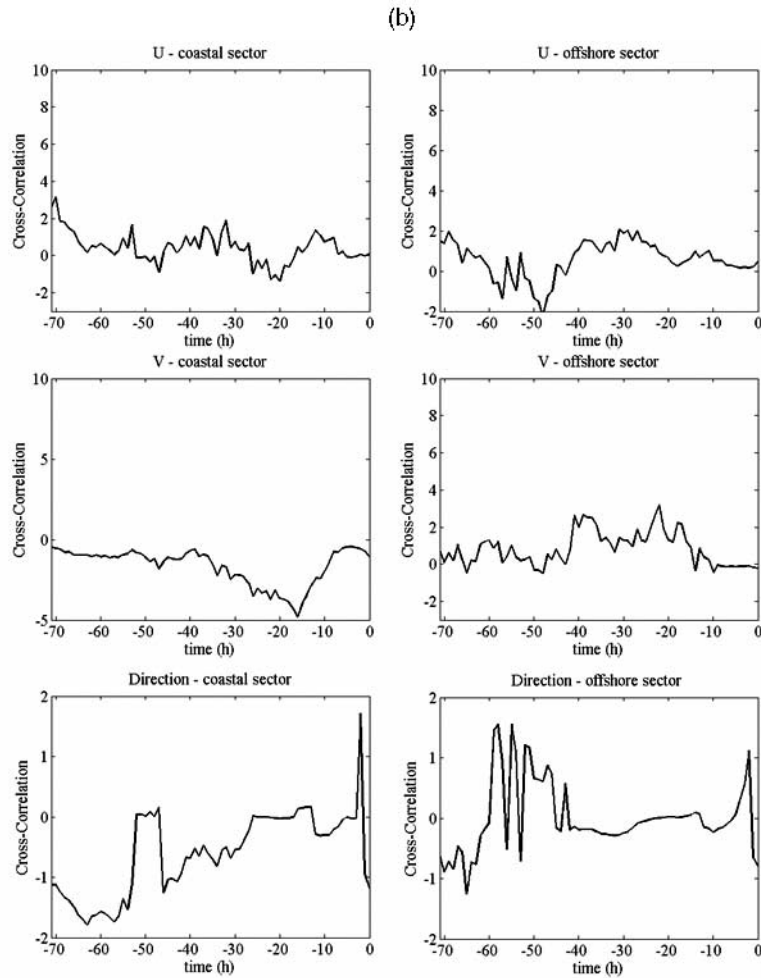
Fig. 9. – *Continued.*

area (Bay of Naples) tend to massively abandon the release area, attaining the offshore sector and sometimes even the domain boundaries. The concentration curves highlight the progressive depletion of tracers (fig. 10a) as typically associated with unidirectional flows [33], with estimated residence times $T^* = 29$ h on average (fig. 10b).

A completely different scenario emerges during westerly wind events. In such conditions, particles launched in open waters are entrapped in the offshore gyres and migrate towards the coast, even though only a limited amount ($\sim 30\%$) enters the Bay of Naples, as shown by $Q(t)$ curves (fig. 11a). On the other hand, almost all tracer particles released in the coastal sector remain in that area being pushed towards the coastline. The flat $Q(t)$ curves (fig. 11b) are indicative of the highly retentive character of this area with the given forcing.

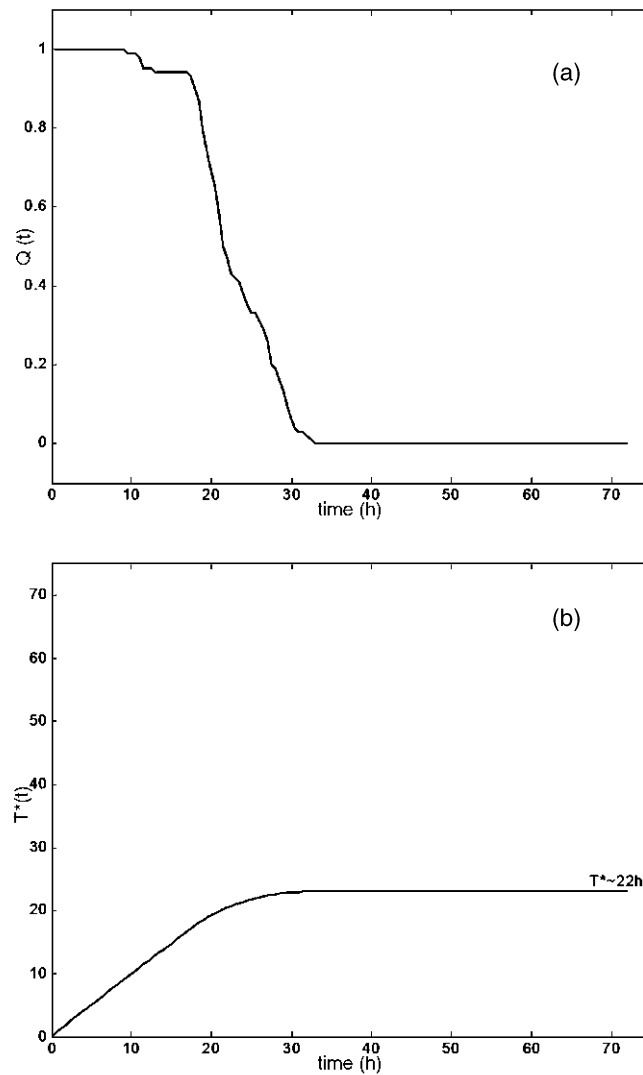A synthetic balance of particle exchanges between offshore and coastal sectors is reported in table II.

Fig. 10. – a) Normalized tracer quantity $Q(t)$ relative to the coastal sector and (b) associated tracer residence time $T^*(t)$ for a period of easterly winds. Tracers released in the Bay of Naples rapidly abandon the launch area, depleting the zone over the three days period. Offshore released particles remain in the outer part of the GoN, often approaching the external boundaries.

8. – Concluding remarks

In this work we have focused on particle exchanges between an offshore and a coastal area of the GoN as driven by the wind acting on the basin during the winter season. Wind is in fact a key local factor in determining the circulation features of the GoN, and consequently in promoting or hampering the renewal of water masses.

On a yearly basis, the wind mainly blows from the NE and SW quadrants, respectively in winter and summer months, while in spring and autumn winds are aligned along the
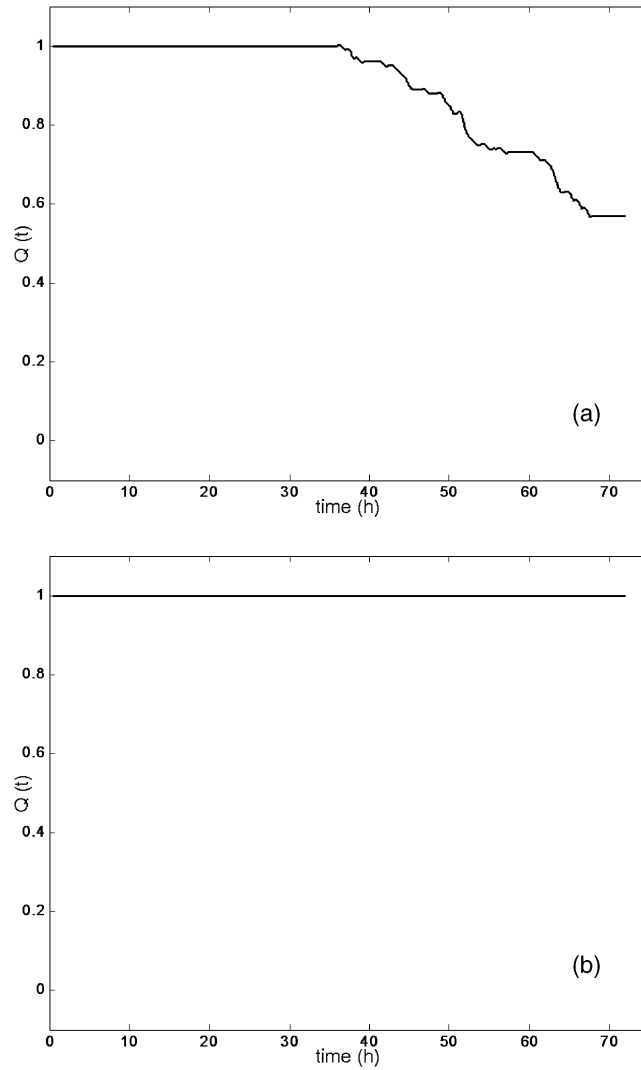
Fig. 11. – a) Normalized tracer quantity $Q(t)$ relative to the coastal sector and (b) to the offshore sector in a westerly wind episode. Most of the particles released offshore remain in the release area, a small amount penetrating in the Bay of Naples, while all particles originated in the inner part of the GoN remain trapped therein.

NNE-SSW axes. In winter months, south-westerly wind periods are also often reported as a consequence of the passage of low-pressure systems associated with cyclonic structures. The circulation in the interior of the GoN is strongly affected by the wind forcing. In the presence of easterlies, the basin scale circulation develops a jet strongly coherent with the wind itself, partly funnelled by the presence of the Vesuvius. On the contrary, in the case of westerlies a lack in coherence between sea surface and wind fields is observed, manifested through the generation of cyclonic and anticyclonic gyres at basin and sub-basin scales. In this latter case, water is pushed onto the coast, a situation likely piling

TABLE II. – *Percentage of exchanged particles between the offshore and the coastal areas in relationship with the wind conditions.*

	Offshore > Coastal area	Coastal area > Offshore
Easterly winds	$\sim 2\%$	$\sim 79\%$
Westerly winds	$\sim 29\%$	$\sim 7\%$

up the sea level in the Bay of Naples [13] and promoting offshore directed counter-currents.

Observed transport is in complete agreement with the above discussed circulation features. The jet associated with the blowing of East winds enhances the offshore-oriented transport from the coast and promotes the export of particles from the domain, sustaining the renewal of water masses (as shown by [14]). By contrast, westerlies enhance the retention features of both the offshore and the coastal areas hampering particle exchange: while many of the particles released in open waters tend to migrate towards the coast, only a portion of them enters the Bay of Naples, while the reduced flushing of this latter sector prevents the tracer particles here originated from abandoning the area.

This study has identified important features in the transport processes in the GoN occurring over short-time periods in wintertime. Future studies will investigate the circulation patters in other periods of the year and explore the seasonality of basin circulation. Our outcomes provide important clues for better understanding the circulation in the basin, as well as the conditions promoting water renewal or particle retention in specific sectors of the basin. In addition, this study confirms the great potential of HF coastal radar systems in providing a rationale by which decision makers may implement specifically targeted operations for the mitigation of the consequences of hazardous events (*e.g.*, oil spills, pollutant discharge) and the implementation of environmentally sustainable actions.

* * *

REFERENCES

[1] GRAVILI D., NAPOLITANO E. and PIERINI S., *Cont. Shelf Res.*, **21** (2001) 455.
[2] MORETTI M., SPEZIE G. and VULTAGGIO M., *Rapp. Comm. int. Mer Médit.*, **27** (1981) 159.
[3] GNRAC, *Lo Stato dei Litorali Italiani - Studi Costieri n°10* (GNRAC, Firenze) 2006.
[4] POVERO P., HOPKINS T. S. and FABIANO M., *Oceanol. Acta*, **13** (1990) 229.

[5] MOREL A., *J. Geophys. Res.*, **93** (1988) 10749.

[6] BRUNET C., CASOTTI R., ARONNE B. and VANTREPOTTE V., *J. Plankton Res.*, **25** (2003) 1413.

[7] CARRADA G. C., HOPKINS T. S., BONADUCE G., IANORA A., MARINO D., MODIGH M., RIBERA D'ALCALÀ M. and SCOTTO DI CARLO B., *PSZNI Mar. Ecol.*, **1** (1980) 105.

[8] RIBERA D'ALCALÀ M., MODIGH M., MORETTI M., SAGGIOMO V., SCARDI M., SPEZIE G. and ZINGONE A., *Oebalia*, XV-1 (1989) 491.

[9] ZINGONE A., MONTRESOR M. and MARINO D., *PSZNI Mar. Ecol.*, **11** (1990) 157.

[10] MORETTI M., SPEZIE G. and VULTAGGIO M., *Rapp. Comm. int. Mer. Médit.*, **28** (1983) 151.

[11] PIERINI S. and SIMIOLI A., *J. Mar. Syst.*, **18** (1998) 161.

[12] MORETTI M., SANSONE E., SPEZIE G., VULTAGGIO M. and DE MAIO A., *Annali Ist. Univ. Nav.*, XLV-XLVI (1977) 207.

[13] DE MAIO A., MORETTI M., SANSONE E., SPEZIE G. and VULTAGGIO M., *Il Nuovo Cimento C*, **8** (1985) 955.

[14] GRIECO L., TREMBLAY L.-B. and ZAMBIANCHI E., *Cont. Shelf Res.*, **25** (2005) 711.

[15] TUKEY J. W., *Exploratory Data Analysis* (Addison-Wesley, Reading, Mass.) 1977.

[16] EBUCHI N., FUKAMACHI Y., OHSHIMA K. I., SHIRASAWA K., ISHIKAWA M., TAKATSUKA T., DAIBO T. and WAKATSUCHI M., *J. Oceanogr.*, **62** (2006) 47.

[17] LIU L., WU X., CHENG F., YANG S. and KE H., *J. Oceanogr.*, **63** (2007) 47.

[18] BARRICK D. E., EVANS M. W. and WEBER B. L., *Science*, **198** (1977) 138.

[19] CROMBIE D. D., *Nature*, **175** (1955) 681.

[20] TRUJILLO D. A., KELLY F. J., PEREZ J. C., RIDDLES H. R. and BONNER J. S., *IEEE J. Ocean. Eng.*, **2** (2004) 1179.

[21] PADUAN J. D. and GRABER H. C., *Oceanography*, **10** (1997) 36.

[22] TEAGUE C. C., VESECKY J. F. and FERNANDEZ D. M., *Oceanography*, **10** (1997) 40.

[23] LIPA B. L., BARRICK D. E., BOURG J. and NYDEN B. B., *J. Oceanogr.*, **62** (2006) 705.

[24] KUNDU P. J., *Fluid Mechanics* (Academic Press, San Diego) 1990.

[25] SMITH S. D., *J. Phys. Oceanogr.*, **10** (1980) 709.

[26] BUFFONI G., FALCO P., GRIFFA A. and ZAMBIANCHI E., *J. Geophys. Res.*, **102** (1997) 699.

[27] CSANADY G. T., *Turbulent Diffusion in the Environment* (D. Reidel Publishing Company, Dordecht) 1980.

[28] FALCO P., GRIFFA A., POULAIN P.-M. and ZAMBIANCHI E., *J. Phys. Oceanogr.*, **30** (2000) 2055.

[29] ESCOFFIER C. and PROVOST C., *Mon. Weather Rev.*, **123** (1995) 1269.

[30] GLICKMAN T. S., *Glossary of Meteorology* (American Meteorological Society, Boston) 2000.

[31] KOSRO P. M., BARTH J. A. and STRUB P. T., *Oceanography*, **10** (1997) 53.

[32] ULLMAN D. S. and CODIGA D. L., *J. Geophys. Res.*, **109** (2004) C07S06.

[33] BELLUCCI A., BUFFONI G., GRIFFA A. and ZAMBIANCHI E., *Dyn. Atmos. Oceans*, **33** (2001) 201.